Stability of scalar spatial solitons in cascadable nonlinear media

A. D. Boardman, K. Xie, and A. Sangarpaul
Photonics and Nonlinear Science Group, Joule Laboratory, Department of Physics, University of Salford, Salford, M5 4WT, United Kingdom

(Received 30 June 1995)

A mathematical stability analysis is presented of the two-beam interactions in quadratic optical nonlinear media that are now attracting such a lot of attention. The averaged Lagrangian is used, within a variational method, and the analysis is based upon a Gaussian trial function. The stability is governed by parameters that can be classified into two groups. One describes spatial solitonlike beam positions and propagation directions and the other describes beam sizes and phases. It is shown that the evolution of these parameters is determined by ten, coupled, ordinary differential equations. The stationary states are proved, mathematically, to be stable for all linear phase mismatch parameter values provided the perturbations are symmetric, i.e., perturbations to beam positions and directions. However, for perturbations to beam sizes or phases, it is proved that a number of stability regimes exist, together with forbidden parameter ranges. The analytical conclusions are completely borne out by computer simulations, and some typical examples are reported here.

PACS number(s): 42.50.Rh, 02.60.Lj, 42.60.Jf, 42.65.Jx

I. INTRODUCTION

Until recently, any discussion of envelope solitons or spatial solitons [1–4] in nonlinear optics was based upon the use of third-order nonlinearity. The general form for the polarization induced by an electromagnetic wave, during its passage through a dielectric material, however, apart from its obvious dependence upon $\chi_{ij}^{(1)}$, the *linear* susceptibility tensor, depends also upon $\chi_{ijk}^{(2)}$, a *second-order* susceptibility tensor, as well as $\chi_{ijkl}^{(3)}$, a *third-order* susceptibility tensor. Truncation at the third order is appropriate for most materials and, furthermore, many elements of these tensors can often be reduced to zero. This means that the tensors are often reduced to a single independent parameter, or at most a small number of independent ones, by the application of the crystal symmetry operations [5,6]. Indeed, it is fortunate that materials needed for real applications are, more often than not, isotropic, amorphous, or possess a rather simple crystal structure. The method of processing the tensors to contain a number of independent elements relies upon the simple fact that crystal structures are invariant with respect to a set of well-known crystal symmetry operations. The lower the symmetry of the material, the smaller the number of these operations becomes. At the highest level, an isotropic, or amorphous, material is invariant to any symmetry operation. The number of nonzero elements of $\chi_{ijk}^{(2)}$ and $\chi_{ijkl}^{(3)}$, as the symmetry falls from the cubic classes down to the triclinic class, can be easily obtained from the literature [5,6], which reveals that there is a basic separation of materials into those that have a center of symmetry and those that do not. The major conclusion is that for nonzero elements of $\chi_{ijk}^{(2)}$ to exist, the material must lack a center of symmetry. This property can be demonstrated only in materials that have not been considered, until recently [7–20], in the context of nonlinear index (soliton) effects. In a $\chi^{(2)}$ material, however, *two* field components can mix to produce a third one that is, once again, at the fundamental frequency, i.e., backmixing occurs, involving the second-harmonic waves and the complex conjugate of the fundamental wave. This recent appreciation of what can happen is dramatic [7,14] and, furthermore, experimental evidence [7] shows that the backmixing (cascading) process is clearly observable, even for large linear phase *mismatching*.

The answer to the question of whether solitons truly exist is complicated, as will be partially illustrated by much of what now follows. In general, a more cautious, *solitonlike*, terminology may be needed, but, if the linear phase-mismatch parameter is large, then the coupled envelope equations for the ω and 2ω waves reduce to a *single* (ω) nonlinear envelope Schrödinger equation and this is called the *cascaded limit*. Obviously, it is this equation that has stable one-dimensional soliton solutions, so choosing to use the word "soliton" to include solutions of the coupled second-harmonic-fundamental wave equations that are *not* in the cascaded limit is a less rigorous terminology.

$\chi^{(2)}$ materials are likely to be in the form of planar waveguides, for which dispersion is generally weak. Diffraction, on the other hand, is strong and is not dependent upon the material [2,3,21]. Furthermore, the scale over which diffraction operates is the order of 1 mm, so the immediate view is that nonlinear beams, for which the tendency to diffract is balanced by nonlinear self-focusing, will be good probes for use in a $\chi^{(2)}$ material. The previous paragraphs highlight the fact that $\chi^{(2)}$ materials, operating in harmonic-fundamental mode or even in *cascaded* (ω) form, are extremely fascinating. They involve very fast nonlinearities [17], with materials that are well known. In principle, they can sustain beams that can be called solitons for a wide range of the linear phase-mismatch parameter.

II. BASIC THEORY

If a dielectric medium supports an electromagnetic wave $\mathbf{E}(\mathbf{r},t)$ that has an angular frequency ω and for which $\mathbf{r}=(x,y,z)$ is a position vector and t is time, then it becomes polarized by an amount $\mathbf{P}\equiv P_i$ $(i=x,y,z)$. The important $\chi^{(2)}$ materials have a single optic axis [5,6] (assumed here to lie along the z axis) and belong to the tetragonal (e.g., $BaTiO_3$), trigonal (e.g., $LiNbO_3$), or hexagonal (e.g., α quartz) systems. These materials are uniaxial and most of the elements of $\chi_{ijk}^{(2)}$ are zero.

For example, $\chi_{ijk}^{(2)}$ for the $\bar{6}$ class of the hexagonal crystal [5,6] system is

$$\chi_{ijk}^{(2)}=\begin{bmatrix} xxx & \overline{xxx} & 0 & 0 & 0 & 0 & 0 & \overline{yyy} & \overline{yyy} \\ \overline{yyy} & yyy & 0 & 0 & 0 & 0 & 0 & \overline{xxx} & \overline{xxx} \\ 0 & 0 & 0 & 0 & 0 & 0 & 0 & 0 & 0 \end{bmatrix}, \quad (1)$$

where the overbar means the negative value and similar expressions for all the crystal classes are readily available [5,6]. Using expressions like (1) in Maxwell's equations leads directly to a description of coupled $(\omega,2\omega)$ two-wave behavior.

The crystal class to which lithium niobate belongs is $3m$ β quartz belongs to 32, barium titanate belongs to $4mm$, and potassium dihydrogen phosphate to $\bar{4}2m$. This paper covers the hexagonal and trigonal systems and hence the associated classes $\bar{6}(C_{3h})$, $\bar{6}m2(D_{3h})$, $32(D_3)$, and $3m(C_{3v})$, where the parentheses contain the Schoenflies symbol. The principal axis of these crystals is along z and this is also the propagation direction. For weakly guided TE or TM waves, the E_z field component is negligible, so only E_x and/or E_y are finite. The terms in $\chi_{ijk}^{(2)}$ that can then feature in the second-order polarization are the (xxx), (xyy), (yxx), (yyy), (yxy), (yyx), (xxy), and (xyx) components. Both E_x and E_y have ω and 2ω parts, which will be defined here as $E_x^{\omega},E_y^{\omega},E_x^{2\omega},E_y^{2\omega}$, and the x component of the second-order polarization is therefore

$$\begin{aligned} P_x^{(2)}=\varepsilon_0\{&\chi_{xxx}^{\omega\omega}E_x^{\omega}E_x^{\omega}+\chi_{xyy}^{\omega\omega}E_y^{\omega}E_y^{\omega}+\chi_{xxx}^{2\omega2\omega}E_x^{2\omega}E_x^{2\omega} \\ &+\chi_{xyy}^{2\omega2\omega}E_y^{2\omega}E_y^{2\omega}+[\chi_{xxx}^{\omega2\omega}+\chi_{xxx}^{2\omega\omega}]E_x^{\omega}E_x^{2\omega} \\ &+[\chi_{xxy}^{\omega\omega}+\chi_{xyx}^{\omega\omega}]E_x^{\omega}E_y^{\omega}+[\chi_{xxy}^{\omega2\omega}+\chi_{xyx}^{2\omega\omega}]E_x^{\omega}E_y^{2\omega} \\ &+[\chi_{xxy}^{2\omega\omega}+\chi_{xyx}^{\omega2\omega}]E_x^{2\omega}E_y^{\omega}+[\chi_{xxy}^{2\omega2\omega}+\chi_{xyx}^{2\omega2\omega}]E_y^{2\omega}E_x^{2\omega} \\ &+[\chi_{xyy}^{\omega2\omega}+\chi_{xyy}^{2\omega\omega}]E_y^{\omega}E_y^{2\omega}\}, \end{aligned} \quad (2)$$

where the notation $\chi_{ijk}^{\omega\omega},\chi_{ijk}^{\omega2\omega}$, has been adopted to keep track of the fundamental and the harmonic wave. In the literature terms such as $(\chi_{xxx}^{\omega2\omega}+\chi_{xxx}^{2\omega\omega})$ are often combined into *one symbol* $\chi_{xxx}^{2\omega\omega}$. The fundamental wave is

$$E_{x,y}^{\omega}=\tfrac{1}{2}[E_{x,y}(\omega)e^{-i\omega t}+\text{c.c.}], \quad (3)$$

where c.c. is the complex conjugate. The same form is to be used for $E_{x,y}^{2\omega}$ and the spatial dependence in $E_{x,y}(\omega)$ and $E_{x,y}(2\omega)$ is implicit. The second-order polarization is

$$P_{x,y}^{(2)}=\tfrac{1}{2}[P_{x,y}^{(2)}(\omega)e^{-i\omega t}+P_{x,y}^{(2)}(2\omega)e^{-i2\omega t}+\text{c.c.}]. \quad (4)$$

After performing all the multiplications, the following forms for $P_x^{(2)}(2\omega)$ and $P_x^{(2)}(\omega)$ are obtained:

$$P_x^{(2)}(2\omega)=\frac{\varepsilon_0}{2}[\kappa_1E_x^2(\omega)-\kappa_1E_y^2(\omega)-2\kappa_2E_x(\omega)E_y(\omega)], \quad (5a)$$

$$\begin{aligned} P_x^{(2)}(\omega)=\frac{\varepsilon_0}{2}[&2\kappa_1E_x^*(\omega)E_x(2\omega)-2\kappa_2E_x^*(\omega)E_y(2\omega) \\ &-2\kappa_2E_y^*(\omega)E_x(2\omega)-2\kappa_1E_y^*(\omega)E_y(2\omega)], \end{aligned} \quad (5b)$$

in which the following definitions have been used:

$$\chi_{xxx}^{\omega\omega}=\chi_{xxx}^{\omega2\omega}=\kappa_1,$$

$$\chi_{xyy}^{\omega2\omega}=\chi_{yxy}^{\omega2\omega}=\chi_{yyx}^{\omega2\omega}=\chi_{xyy}^{\omega\omega}=\chi_{yxy}^{\omega\omega}=\chi_{yyx}^{\omega\omega}=-\kappa_1,$$

$$\chi_{yyy}^{\omega\omega}=\chi_{yyy}^{\omega2\omega}=\kappa_2,$$

$$\chi_{yxx}^{\omega2\omega}=\chi_{xyx}^{\omega2\omega}=\chi_{xxy}^{\omega2\omega}=\chi_{xxy}^{\omega\omega}=\chi_{yxx}^{\omega\omega}=\chi_{xyx}^{\omega\omega}=-\kappa_2.$$

In Eq. (2) coefficients such as $\chi_{xxx}^{\omega2\omega}+\chi_{xxx}^{2\omega\omega}$ were not rolled into *one coefficient* $\chi_{xxx}^{\omega2\omega}$, so this is why $\chi_{xxx}^{\omega\omega}=\chi_{xxx}^{\omega2\omega}$, etc. κ_1 and κ_2 are associated with the symmetry groups and associated classes, in the following way: for the hexagonal system,

$$\kappa_1\neq\kappa_2\neq0 \quad (\bar{6}\ \text{class}),$$

$$\kappa_1=0 \quad (\bar{6}m2\ \text{class}),$$

and for the trigonal system,

$$\kappa_2=0 \quad (32\ \text{class}),$$

$$\kappa_1=0 \quad (3m\ \text{class}).$$

There are similar expressions for $P_y^{(2)}(2\omega)$ and $P_y^{(2)}(\omega)$. Taken together, Eqs. (5) and the corresponding expressions for $P_y^{(2)}(2\omega)$ and $P_y^{(2)}(\omega)$ are very interesting. they show that, depending upon the values of κ_1 and κ_2, even if E_x is initially set to zero, E_y *drives* P_x so E_x will start to grow. The same argument applies to E_y. This means that the choice of symmetry group is important. For example, if $\kappa_1=0(\bar{6}m2,3m)$, then setting $E_x=0$ permits E_y (TM wave) to exist by itself without a driving term causing E_x to appear. On the other hand, if $\kappa_1\neq0$ then sustaining $E_x=0$ is impossible since E_y is finite and *drives* P_x.

The material will be assumed to be in the form of a planar waveguide. Propagation is along the z axis, guiding is in the y direction, and the balancing of diffraction with nonlinear focusing takes place, in the plane of the guide, in the $\pm x$ directions. The field components are essentially uniform in the y direction, with weak guiding, meaning that a TM has only an E_y component, while a TE wave has only an E_x component.

If the beams are TE polarized $\mathbf{E}(\omega)=\hat{\mathbf{x}}E_{\omega}$ and $\mathbf{E}(2\omega)=\hat{\mathbf{x}}E_{2\omega}$, where $\hat{\mathbf{x}}$ is a unit vector, the nonlinear polarizations, for the 32 class, are

$$P_x^{(2)}(2\omega)\equiv P_{2\omega}^{(2)}=\frac{\varepsilon_0\kappa_1}{2}E_{\omega}^2, \quad (6a)$$

$$P_x^{(2)}(\omega)\equiv P_{\omega}^{(2)}=\varepsilon_0\kappa_1E_{\omega}^*E_{2\omega}. \quad (6b)$$

The equations for $E(\omega)$ and $E(2\omega)$ are

$$\frac{\partial^2 E_\omega}{\partial z^2}+\frac{\partial^2 E_\omega}{\partial x^2}+\frac{\omega^2}{c^2}\varepsilon_\omega E_\omega+\frac{\omega^2}{c^2}\kappa_1 E_\omega^* E_{2\omega}=0, \tag{7a}$$

$$\frac{\partial^2 E_{2\omega}}{\partial z^2}+\frac{\partial^2 E_{2\omega}}{\partial x^2}+\left(\frac{2\omega}{c}\right)^2\varepsilon_{2\omega}E_{2\omega}+\frac{1}{2}\left(\frac{2\omega}{c}\right)^2\kappa_1 E_\omega^2=0, \tag{7b}$$

where $\varepsilon_\omega=n^2(\omega)$ and $\varepsilon_{2\omega}=n^2(2\omega)$ are the *linear* dielectric functions at frequencies ω and 2ω, and $n(\omega)$ and $n(2\omega)$ are the respective refractive indices.

It is convenient now to emphasize the slow variation of the amplitudes E_ω and $E_{2\omega}$ on z. This is done by factoring out the fast z dependence by writing $E_\omega=E_1(x,z)\exp[i(k_\omega z-\omega t)]$ and $E_{2\omega}=E_2(x,z)\exp[i(k_{2\omega}z-2\omega t)]$, defining $E_1\equiv E_1(x,z)$ and $E_2\equiv E_2(x,z)$, and, finally, making $k_\omega|\partial E_1/\partial z|\gg|\partial^2 E_1/\partial z^2|$ and $k_{2\omega}|\partial E_2/\partial z|\gg|\partial^2 E_2/\partial z^2|$. The fact that $k_\omega=(\omega/c)\sqrt{\varepsilon_\omega}$ and $k_{2\omega}=(2\omega/c)\sqrt{\varepsilon_{2\omega}}$ are the linear wave numbers means that the linear phase mismatch is $\Delta k=k_{2\omega}-2k_\omega$. The further definitions $E_1(w/\sqrt{2})\exp(i\beta_1 z)$ and $E_2=v\exp(i\beta_2 z)$, the transformations $(\omega/c)^2(w\kappa_1/2k_\omega\beta_1)\to w$, $(\omega/c)^2(v\kappa_1/2k_\omega\beta_1)\to v$, $\sqrt{2k_\omega\beta_1}x\to x$, and $\beta_1 z\to z$, and the choice $\Delta k+\beta_2-2\beta_1=0$ result in a reduction of the coupled equations to

$$i\frac{\partial w}{\partial z}+\frac{\partial^2 w}{\partial x^2}-w+w^*v=0, \tag{8a}$$

$$i2\alpha\frac{\partial v}{\partial z}+\frac{\partial^2 v}{\partial x^2}-\alpha\beta v+w^2=0, \tag{8b}$$

where $\beta=2\beta_2/\beta_1$ and $\alpha=k_{2\omega}/2k_\omega=\sqrt{\varepsilon_{2\omega}/\varepsilon_\omega}$ is the linear phase-mismatch parameter. The development leading to Eqs. (8), based, as it is, upon the use of crystal symmetry, shows clearly how the coupled scalar equations arise. Nevertheless, the specific form of Eqs. (8) can be found in a recent publication [18] provided that the following identifications are made in [18]: $\alpha\to\alpha\beta$ and x is scaled as $\sqrt{k_\omega\beta_1}x\to x$. The scaling of w and v in [18] is equivalent to Eqs. (8). The resolution of E_1 and E_2 into slowly varying parts w and v and fast dependences $\exp(i\beta_1 z)$ and $\exp(i\beta_2 z)$ is interesting. In the nonstationary regimes w and v are complex but, for stationary states, w and v are real and independent of z, while β_1 and β_2 are *exactly* the nonlinear phase shifts. This canonical form of the nonlinear equations describes the competition between diffraction and nonlinearity during the copropagation of the second-harmonic wave and the fundamental wave. They are not restricted to a near phase-matching limit ($\alpha\cong 1$), so neither (2a) nor (2b) is a nonlinear Schrödinger equation. This means that exact soliton solutions must not be expected as stationary states. Solitonlike solutions should be possible; however, some may well be stable. True solitons will certainly appear in the *cascaded* limit $|\alpha\beta v|\gg|2\alpha(\partial v/\partial z)|,|\partial^2 v/\partial x^2|$. This cascaded limit gives $v=w^2/\alpha\beta$ and recovers the nonlinear Schrödinger equation

$$i\frac{\partial w}{\partial z}+\frac{\partial^2 w}{\partial x^2}-w+\frac{1}{\alpha\beta}|w|^2 w=0. \tag{9}$$

An effective mass

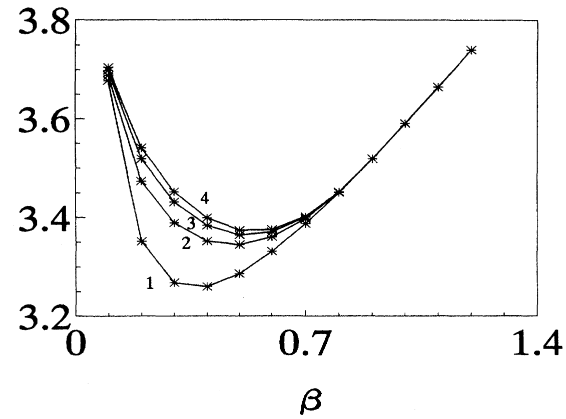

FIG. 1. Variation of the effective mass M with β, the nonlinear phase-mismatch parameter. $\alpha=1.01$ and the true mass has been divided by the number of peaks in the field distribution to put all the graphs onto a similar scale. The graphs are labeled with the number of peaks.

$$M=\frac{1}{\sqrt{2\pi}}\int\left[\tfrac{1}{2}|w|^2+\alpha|v|^2\right]dx \tag{10}$$

can be defined through Eq. (4). Viewing the eigenstates as "particles," this is a constant of "the motion" with the other conserved quantities being the *momentum*

$$P=\frac{i}{\sqrt{2\pi}}\int\left[w\frac{\partial w^*}{\partial x}-w^*\frac{\partial w}{\partial x}+\alpha v\frac{\partial v^*}{\partial x}-\alpha v^*\frac{\partial v}{\partial x}\right]dx \tag{11}$$

and the *Hamiltonian*

$$H=\left(\frac{2}{\pi}\right)^{1/2}\int\left[\left|\frac{\partial w}{\partial x}\right|^2+\frac{1}{2}\left|\frac{\partial v}{\partial x}\right|^2+|w|^2+\frac{\alpha}{2}\beta|v|^2-\frac{1}{2}(w^{*2}v+w^2v^*)\right]dx. \tag{12}$$

For stationary solutions $\partial w/\partial z=\partial v/\partial z=0$ and the coupled equations reduce to

$$\frac{d^2 w}{dx^2}-w+wv=0, \tag{13a}$$

$$\frac{d^2 v}{dx^2}-\alpha\beta v+w^2=0. \tag{13b}$$

These coupled equations can be integrated once [18] to give

$$\frac{1}{2}\left(\frac{dw}{dx}\right)^2+\frac{1}{4}\left(\frac{dv}{dx}\right)^2+\frac{1}{2}\left(w^2v-\frac{\alpha\beta}{2}v^2-w^2\right)=C,$$

where C is a constant of integration. The case $C=0$ corresponds to a soliton solution. Equations (13) do not yield any more conservation laws and analytical solutions can only be found for certain values of $\alpha\beta$. For example, it is easy to show that $w=v=\frac{3}{2}\mathrm{sech}^2(x/2)$ for $\alpha\beta=1$, but, in general, Eqs. (13a) and (13b) have to be solved numerically. Figure 1 shows the variation of effective mass [Eq. (10)] with β for

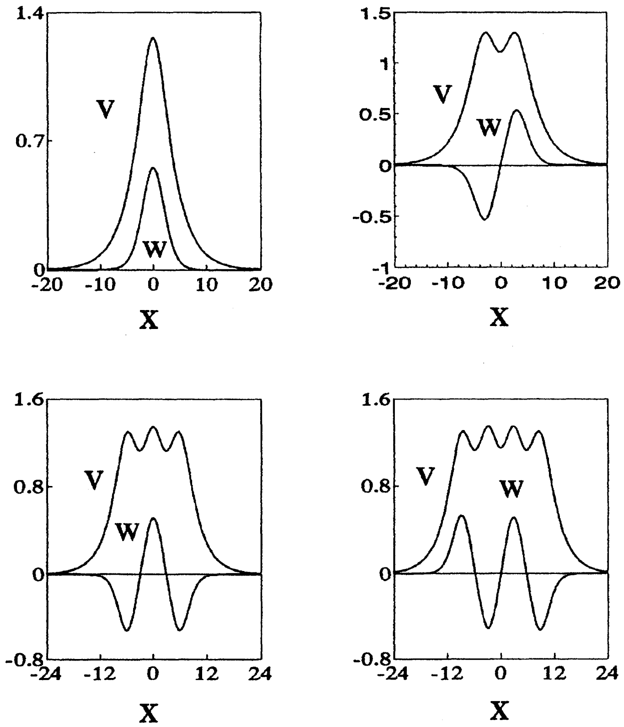

FIG. 2. Typical symmetric and antisymmetric field profiles.

two different types of symmetric and antisymmetric soliton-like solutions when $\alpha = 1.01$. Typical forms of the solutions are displayed in Fig. 2. The single-peak solution has been reported earlier [17], but the antisymmetric soliton solutions are interesting because, for these solutions, the v component is still symmetric in x, while the w component is antisymmetric about $x=0$.

Since the original coupled equations are not integrable, vital properties of their solutions such as their stability and the kind of initial conditions that will result in a soliton cannot be discovered by direct mathematics. No stability for multipeak solutions has been found numerically, but, for some parameter values, single-peak solutions appear to be stable. It is important, therefore, to investigate these single-peak solutions in some detail so that their stability regimes can be precisely defined. It is clear that general conclusions cannot be drawn from an inevitably small number of numerical experiments, so, in the following, a variational method will be used to analyze the stability of the fundamental solitary single-peak wave.

III. STABILITY ANALYSIS

In $\chi^{(2)}$ material there is both a fundamental beam (at ω) and a harmonic beam (at 2ω), which are copropagating. What will be done here is to investigate the consequences of a perturbation to beam position and direction, on the one hand, and a perturbation to beam size and phase, on the other. The first kind of perturbation represents a mismatch, in position or direction, between the fundamental and the harmonic wave, at the moment of launching. The second type represents an energy or phase fluctuation. The stability analysis begins with the Lagrangian density [2,3,21] for the coupled (v,w) equations, which is

$$L=\frac{i}{2}\left(w^*\frac{\partial w}{\partial z}-w\frac{\partial w^*}{\partial z}\right)+\frac{i\alpha}{2}\left(v^*\frac{\partial v}{\partial z}-v\frac{\partial v^*}{\partial z}\right)-\left|\frac{\partial w}{\partial x}\right|^2 -|w|^2-\frac{1}{2}\left|\frac{\partial v}{\partial x}\right|^2-\frac{\alpha\beta}{2}|v|^2+\frac{1}{2}(w^{*2}v+w^2v^*). \tag{14}$$

At this point some trial functions must be introduced and the ones selected are Gaussian, simply because they are very convenient. They are

$$w=\eta_1\exp\left[-\rho_1^2(x-x_1)^2+i\frac{\xi_1}{2}(x-x_1)+i\frac{\theta_1}{2}\right], \tag{15a}$$

$$v=\eta_2\exp[-\rho_2^2(x-x_2)^2+i\xi_2(x-x_2)+i\theta_2], \tag{15b}$$

where $\eta_{1,2}$ are amplitudes, $\rho_{1,2}$ are inverse beam widths, $\xi_{1,2}$ are beam propagation directions, $x_{1,2}$ are the beam centers, and $\theta_{1,2}$ are phases.

The reduced Lagrangian is [22]

$$\mathscr{L}=\left(\frac{2}{\pi}\right)^{1/2}\int L\,dx=\mathscr{L}_1+\mathscr{L}_2+\mathscr{L}_{12}, \tag{16}$$

where $\mathscr{L}_1$, $\mathscr{L}_2$, and $\mathscr{L}_{12}$ need not be formally identified at this stage. The Euler-Lagrange equations are

$$\frac{\partial\mathscr{L}}{\partial g}-\frac{d}{dz}\left[\frac{\partial\mathscr{L}}{\partial(\partial g/\partial z)}\right]=0, \tag{17}$$

where $g=\eta_i,\rho_i,\theta_i,\xi_i$ $(i=1,2)$. Generating useful nonlinear, ordinary, coupled equations for the parameters in (15) is a straightforward use of Eq. (17) but does involve *considerable labor.* A typical equation is

$$-\alpha\frac{\eta_2^2}{\rho_2^2}\xi_2\frac{dx_2}{dz}+\alpha\frac{\eta_2^2}{\rho_2^2}\frac{d\theta_2}{dz}-\frac{\eta_2^2}{2}+\frac{\eta_2^2}{2\rho_2^2}\xi_2^2 +\frac{\alpha\beta}{2}\frac{\eta_2^2}{\rho_2^2}+\frac{\partial\mathscr{L}_{12}}{\partial\rho_2}=0, \tag{18}$$

where

$$\mathscr{L}_{12}=\left(\frac{2}{\pi}\right)^{1/2}\eta_1^2\eta_2\int\exp[-2\rho_1^2(x-x_1)^2-\rho_2^2(x-x_2)^2] \times\cos[\theta_2-\theta_1+\xi_2(x-x_2)-\xi_1(x-x_1)]dx. \tag{19}$$

The Hamiltonian of the system is

$$H=\rho_1\eta_1^2+\frac{\eta_1^2}{4\rho_1}\xi_1^2+\frac{\eta_1^2}{\rho_1}+\frac{1}{2}\rho_2\eta_2^2+\frac{\eta_2^2}{2\rho_2}\xi_2^2+\frac{\alpha\beta}{2}\frac{\eta_2^2}{\rho_2}-\mathscr{L}_{12}. \tag{20}$$

A. Stationary solitary solitons

A stationary solution occurs whenever $dx_1/dz = dx_2/dz=0$, $d\xi_1/dz=d\xi_2/dz=0$, $d\theta_1/dz=d\theta_2/dz=0$, and $(d/dz)(\eta_1^2/2\rho_1)=(d/dz)(\eta_2^2/\rho_2)=0$. Such conditions demand that $x_1=x_2=0$, $\xi_1=\xi_2=0$, $\theta_1=\theta_2=0$, $\eta_1=\eta_{10}$, $\eta_2=\eta_{20}$, $\rho_1=\rho_{10}$, $\rho_2=\rho_{20}$, and $\rho_{10},\rho_{20},\eta_{10},\eta_{20}$ satisfy the equations

$$(\rho_{10}^2+1)^2(2\rho_{10}^2+\rho_{20}^2)=2\rho_{10}^2\eta_{20}^2, \tag{21a}$$

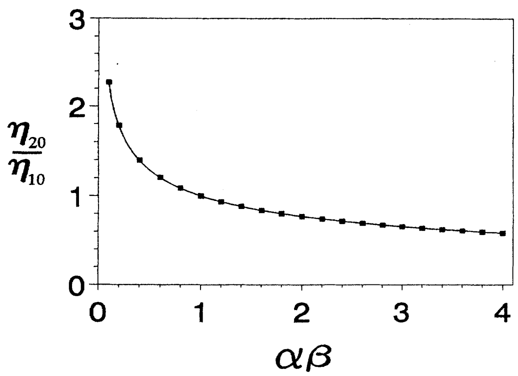

FIG. 3. Ration of second-harmonic wave amplitude to the fundamental wave amplitude, as a function of $\alpha\beta$. ■—■, exact numerical result; ——, variational calculation.

$$(\rho_{20}^2+\alpha\beta)^2(2\rho_{10}^2+\rho_{20}^2)=2\rho_{20}^2\eta_{10}^4/\eta_{20}^2, \tag{21b}$$

$$(-\rho_{10}^2+1)(2\rho_{10}^2+\rho_{20}^2)=2\rho_{10}^2(\rho_{10}^2+1), \tag{21c}$$

$$(-\rho_{20}^2+\alpha\beta)(2\rho_{10}^2+\rho_{20}^2)=2\rho_{20}^2(\rho_{20}^2+\alpha\beta). \tag{21d}$$

If $\alpha\beta=1$, then $\eta_{10}=\eta_{20}=\frac{3}{5}\sqrt{6}$, $\rho_{10}=\rho_{20}=1/\sqrt{5}$, and $w=v=(3\sqrt{6}/5)\exp(-x^2/5)$. This solution is extremely close to the *special exact value* [17], which is $\frac{3}{2}\text{sech}^2(x/2)$. For general $\alpha\beta$, a cubic equation in ρ_{10}^2 can be obtained, i.e.,

$$\rho_{10}^6+\left(\frac{4-3\alpha\beta}{20}\right)\rho_{10}^4+\frac{\alpha\beta}{5}\rho_{10}^2-\frac{\alpha\beta}{20}=0. \tag{22}$$

Only a positive real root of Eq. (22) has any physical meaning, and when $\alpha\beta<0$ this real root becomes negative and the system will not sustain a solitary wave. Once Eq. (22) is solved ρ_{20}, η_{10}, and η_{20} are easily found from

$$\rho_{20}^2=4\rho_{10}^4/(1-\rho_{10}^2), \tag{23a}$$

$$\eta_{10}^2=\frac{(2\rho_{10}^2+\rho_{20}^2)}{2\rho_{10}\rho_{20}}(\rho_{10}^2+1)(\rho_{20}^2+\alpha\beta), \tag{23b}$$

$$\eta_{20}^2=\frac{(2\rho_{10}^2+\rho_{20}^2)}{2\rho_{10}^2}(\rho_{10}^2+1)^2. \tag{23c}$$

The ratio of η_{20}/η_{10} that is needed to sustain a coupled $(2\omega,\omega)$ solitary wave is obtainable from Eqs. (23) as a function of $\alpha\beta$. This is plotted in Fig. 3, together with the exact numerical solutions. It can be seen that the mathematical results, based upon the variational analysis, and the exact numerical results coincide, for all practical purposes.

B. Beam position and direction perturbations

In this case, the mismatch in position or direction of the fundamental and harmonic wave, at the moment of launching, can be expressed as follows. The equilibrium (stationary state) positions are $x_1=x_2=0$ and $\xi_1=\xi_2=0$, so a disturbance to this state will now be defined as $x_1=\delta x_1$, $x_2=\delta x_2$, $\xi_1=\delta\xi_1$, and $\xi_2=\delta\xi_2$, where all the perturbations are small. The evolution equations, obtained from the Euler-Lagrange equations, involve only x_1, x_2, ξ_1, and ξ_2. All the other equations yield nothing, as expected. If the two variables $\alpha(\eta_{20}^2/\rho_{20})\xi_2-(\eta_{10}^2/2\rho_{10})\xi_1=2M\xi$ and $x_2-x_1=\Delta$, where $2M=\alpha(\eta_{20}^2/\rho_{20})+(\eta_{10}^2/2\rho_{10})$ is the total mass, are used, then the evolution equations reduce to

$$\frac{d\Delta}{dz}=\left[\frac{1}{\alpha}\frac{\rho_{20}}{\alpha\eta_{20}^2}+\frac{2\rho_{10}}{\eta_{10}^2}+\frac{\sqrt{2}}{2}\frac{\eta_{10}^2\eta_{20}}{(2\rho_{10}^2+\rho_{20}^2)^{3/2}}\times\left(\frac{\rho_{20}}{\alpha\eta_{20}^2}+\frac{2\rho_{10}}{\eta_{10}^2}\right)^2\right]M\xi=a\xi, \tag{24}$$

$$\frac{d\xi}{dz}=-4\sqrt{2}\frac{\eta_{10}^2\eta_{20}}{(2\rho_{10}^2+\rho_{20}^2)^{3/2}}\rho_{10}^2\rho_{20}^2\frac{\Delta}{M}=-b\Delta. \tag{25}$$

Hence

$$\frac{1}{2}\left(\frac{d\Delta}{dz}\right)^2+\frac{ab}{2}\Delta^2=0,\quad \frac{1}{2}\left(\frac{d\xi}{dz}\right)^2+\frac{ab}{2}\xi^2=0. \tag{26}$$

Since $a>0$ and $b>0$ the potentials $U(\Delta)=(ab/2)\Delta^2$ and $U(\xi)=(ab/2)\xi^2$ are always *concave* at $\xi=0$ and $\Delta=0$. The conclusion is that the stationary solutions are *always stable* when subjected to this type of perturbation and this is true for all $\alpha\beta$.

C. Beam size and phase perturbations

For this type of perturbation ξ_1, ξ_2, x_1, and x_2 remain at their initial values, zero in this case. The perturbation drives ρ_i to $\rho_{i0}+\delta\rho_i$ $(i=1,2)$ and θ_1 and θ_2 shift from zero to become $\theta_1=\delta\theta_1$ and $\theta_2=\delta\theta_2$.

The perturbation will be characterized below with the new variables $N_1=\eta_1^2/2\rho_1$ and $N_2=\eta_2^2/\rho_2$, so that $\delta\eta_1=(\rho_{10}/\eta_{10})\delta N_1+(\eta_{10}/2\rho_{10})\delta\rho_1$, for example. N_1 and N_2 represent the total energy in the fundamental and the harmonic, respectively. First, the Euler-Lagrange equations generate the differential equations

$$\frac{d}{dz}\left(\frac{\eta_1^2}{2\rho_1}\right)=-\frac{\sqrt{2}\eta_1^2\eta_2}{\sqrt{2\rho_1^2+\rho_2^2}}\sin(\theta_2-\theta_1), \tag{27a}$$

$$\alpha\frac{d}{dz}\left(\frac{\eta_2^2}{\rho_2}\right)=+\frac{\sqrt{2}\eta_1^2\eta_2}{\sqrt{2\rho_1^2+\rho_2^2}}\sin(\theta_2-\theta_1), \tag{27b}$$

$$\frac{d\theta_1}{dz}=-2\rho_1^2-2+2\sqrt{2}\frac{\rho_1\eta_2}{\sqrt{2\rho_1^2+\rho_2^2}}\cos(\theta_2-\theta_1), \tag{27c}$$

$$\alpha\frac{d\theta_2}{dz}=-\frac{\rho_2^2}{2}-\frac{\alpha\beta}{2}+\frac{\sqrt{2}}{2}\frac{\rho_2\eta_1^2/\eta_2}{\sqrt{2\rho_1^2+\rho_2^2}}\cos(\theta_2-\theta_1) \tag{27d}$$

and the algebraic equations

$$2\rho_1^2(2\rho_1^2+\rho_2^2)^3=\rho_2^4\eta_2^2\cos^2(\theta_2-\theta_1), \tag{28a}$$

$$\rho_1\eta_1^2(2\rho_1^2-\rho_2^2)=\rho_2^3\eta_2^2. \tag{28b}$$

Substituting the perturbed quantities and keeping only the lowest order in $\delta\rho_1$, $\delta\rho_2$, δN_1, δN_2, $\delta\theta_1$, and $\delta\theta_2$ gives

$$\frac{d}{dz}\delta N_1 = -a(\theta_2-\theta_1), \quad \alpha\frac{d}{dz}\delta N_2 = a(\theta_2-\theta_1), \tag{29a}$$

$$\frac{d}{dz}\delta\theta_1 = b_1\delta\rho_1 + b_2\delta\rho_2 + b_3\delta N_2,$$

$$\frac{d}{dz}\delta\theta_2 = b_4\delta\rho_1 + b_5\delta\rho_2 + b_6\delta N_1 + b_7\delta N_2, \tag{29b}$$

where $a=\sqrt{2}\eta_{10}^2\eta_{20}/\sqrt{2\rho_{10}^2+\rho_{20}^2}$ and $b_1,\ldots,b_7$ require some effort to obtain, but can be obtained in a relatively straightforward way. Explicitly,

$$b_1 = -4\rho_{10} + \frac{2\sqrt{2}\rho_{10}\eta_{20}}{\sqrt{2\rho_{10}^2+\rho_{20}^2}}\left(\frac{1}{\rho_{10}} - \frac{2\rho_{10}}{2\rho_{10}^2+\rho_{20}^2}\right), \tag{30a}$$

$$b_2 = \frac{2\sqrt{2}\rho_{10}\eta_{20}}{\sqrt{2\rho_{10}^2+\rho_{20}^2}}\left(\frac{1}{2\rho_{20}} - \frac{\rho_{20}}{2\rho_{10}^2+\rho_{20}^2}\right),$$

$$b_3 = \frac{\sqrt{2}\rho_{10}}{\sqrt{2\rho_{10}^2+\rho_{20}^2}}\frac{\rho_{20}}{\eta_{20}}, \tag{30b}$$

$$b_4 = \frac{\sqrt{2}}{2\alpha}\frac{\rho_{20}\eta_{10}^2/\eta_{20}}{\sqrt{2\rho_{10}^2+\rho_{20}^2}}\left(\frac{1}{\rho_{10}} - \frac{2\rho_{10}}{2\rho_{10}^2+\rho_{20}^2}\right),$$

$$b_5 = -\frac{\rho_{20}}{\alpha} + \frac{\sqrt{2}}{2\alpha}\frac{\rho_{20}\eta_{10}^2/\eta_{20}}{\sqrt{2\rho_{10}^2+\rho_{20}^2}}\left(\frac{1}{2\rho_{20}} - \frac{2\rho_{20}}{2\rho_{10}^2+\rho_{20}^2}\right), \tag{30c}$$

$$b_6 = \frac{\sqrt{2}\rho_{10}\rho_{20}/\eta_{20}}{\alpha\sqrt{2\rho_{10}^2+\rho_{20}^2}}, \quad b_7 = -\frac{\sqrt{2}}{4\alpha}\left[\frac{\rho_{20}^2\eta_{10}^2/\eta_{20}^3}{\sqrt{2\rho_{10}^2+\rho_{20}^2}}\right]. \tag{30d}$$

$\delta\rho_1$ and $\delta\rho_2$ are related to δN_1 and δN_2 by the equations

$$\delta\rho_1 = b_8\delta N_1 + b_9\delta N_2, \tag{31a}$$

$$\delta\rho_2 = b_{10}\delta N_1 + b_{11}\delta N_2, \tag{31b}$$

where

$$b_8 = \frac{\rho_{10}^2}{3\eta_{10}^2}\left(\frac{2\rho_{10}^2-\rho_{20}^2}{2\rho_{10}^2+\rho_{20}^2}\right)\left(\frac{10\rho_{10}^2-\rho_{20}^2}{4\rho_{10}^2-\rho_{20}^2}\right),$$

$$b_9 = \frac{\rho_{10}\rho_{20}}{6\eta_{20}^2}\left[\frac{-4\rho_{10}^4+16\rho_{10}^2\rho_{20}^2-3\rho_{20}^4}{(2\rho_{10}^2+\rho_{20}^2)(4\rho_{10}^2-\rho_{20}^2)}\right], \tag{32a}$$

$$b_{10} = \frac{2\rho_{10}\rho_{20}}{3\eta_{10}^2}\left(\frac{2\rho_{10}^2-\rho_{20}^2}{2\rho_{10}^2+\rho_{20}^2}\right)\left(\frac{8\rho_{10}^2+\rho_{20}^2}{4\rho_{10}^2-\rho_{20}^2}\right),$$

$$b_{11} = -\frac{8\rho_{10}\rho_{20}}{3\eta_{20}^2}\left[\frac{\rho_{10}\rho_{20}(\rho_{10}^2-\rho_{20}^2)}{(2\rho_{10}^2+\rho_{20}^2)(4\rho_{10}^2-\rho_{20}^2)}\right]. \tag{32b}$$

It is now easy to show that $(d/dz)(\delta N_1+\delta N_2)=0$, so that it is safe to choose $\delta N_1+\delta N_2=0$ as an initial value. After adopting the definitions $2N=\delta N_2-\delta N_1$ and $\theta=\theta_2-\theta_1$, the evolution of this kind of perturbation is described by the simple equations

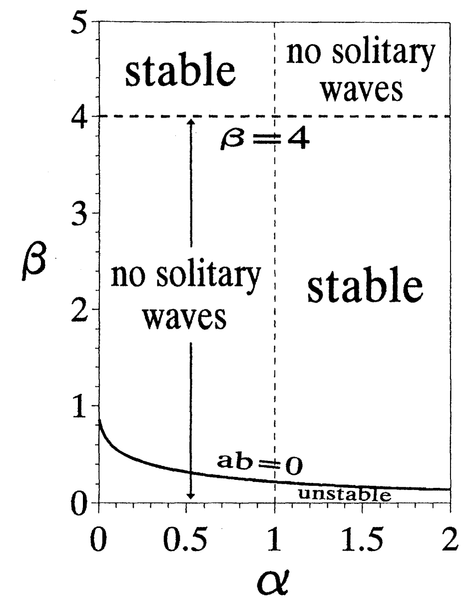

FIG. 4. Stability and existence regions of the (β,α) plane, for single-peak solutions.

$$\frac{dN}{dz} = a\theta, \tag{33}$$

$$\frac{d\theta}{dz} = -bN, \tag{34}$$

where $b=(b_4-b_1)(b_8-b_9)+(b_5-b_2)(b_{10}-b_{11})+b_3+b_6-b_7$. The coupled equations (33) and (34) give

$$\frac{1}{2}\left(\frac{dN}{dz}\right)^2 + U(N)=0, \quad \frac{1}{2}\left(\frac{d\theta}{dz}\right)^2 + U(\theta)=0, \tag{35}$$

where

$$\left(\frac{d^2U(N)}{dN^2}\right)_{N=0} = \left(\frac{d^2U(\theta)}{d\theta^2}\right)_{\theta=0} = ab$$

determines the shape of the potential functions $U(N)$ and $U(\theta)$ at the origin $(N=0,\ \theta=0)$.

For $ab>0$, $d^2U/dN^2=d^2U/d\theta^2>0$ and the stationary solutions can be stable. For $ab<0$, however, all solitary wave solutions are unstable. Figure 4 shows the stability regions on the (β,α) plane. The figure shows that there are a number of domains in which solitary waves can exist, but not all of them are stable. The boundary $ab=0$ is drawn in Fig. 4 because this condition emerged from the above stability analysis. In addition, the nonlinear phase-matching condition is $2k_\omega-k_{2\omega}-\beta_2+2\beta_1=0$, so this must also be taken into account when defining the existence regimes of the solitary waves. The crucial point here is that $\beta_1>0$, $\beta_2>0$, and $\alpha\beta>0$ so the phase-matching condition is

$$\beta_1 = 4k_\omega\frac{1-\alpha}{\beta-4}, \quad \beta_2 = 2k_\omega\beta\frac{1-\alpha}{\beta-4}. \tag{36}$$

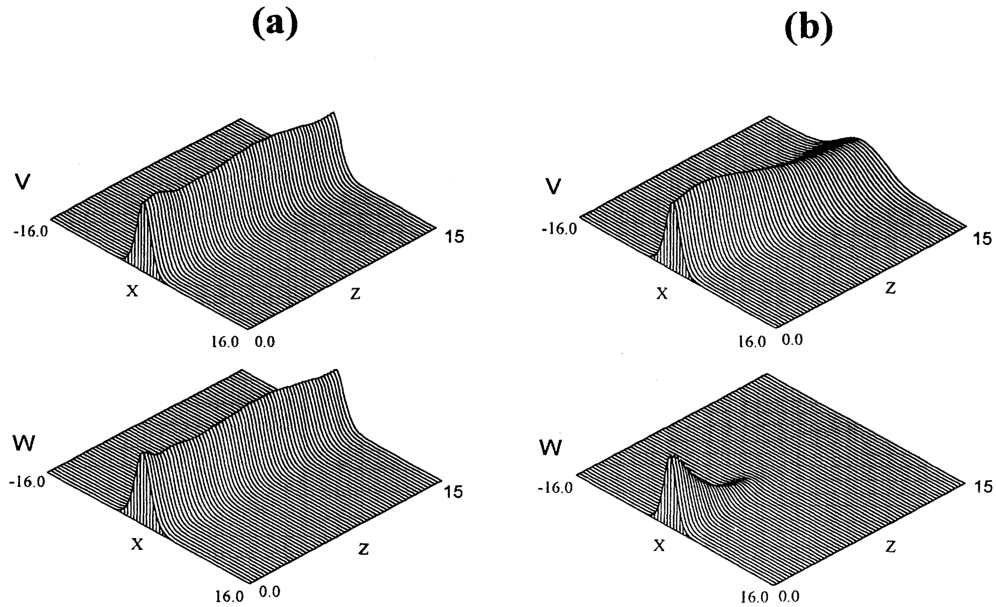

FIG. 5. Numerical simulations of the behavior of single-peak coupled waves. The simulations show the propagation behavior of v (harmonic) and w (fundamental) for (a) $(\beta,\alpha)=(2.0,1.01)$ and (b) $(\beta,\alpha)=(0.2,1.01)$.

The linear phase-matching point $\alpha=1$ separates the regions in which $1-\alpha$ is positive or negative. For example, if $\alpha>1$, then $1-\alpha<0$, so that it is necessary to have $\beta-4<0$ to keep $\beta_{1,2}>0$. A *second* boundary line on the (β,α) plot, for $\beta=4$, must be drawn, so the division of the (β,α) plane into permitted solitary wave solutions is more complicated than that defined by $ab=0$. As $\beta\rightarrow4$, $\beta_{1,2}\rightarrow\infty$, so the line $\beta=4$ for a given α separates out the regions where nonlinear phase matching is possible. In this sense, the line defined by $\beta=4$ could be called the nonlinear phase-matching edge. Clearly, with $\beta_{1,2}\rightarrow\infty$, as $\beta\rightarrow4$ it will require more and more power to drive such a state. Figure 5 contains numerical simulations that provide an exact verification of the stability conclusions by sampling a few parameter values.

IV. CONCLUSIONS

The ideas involved in cascaded nonlinearity are clearly exposed through a study of scalar waves. The involvement of crystal symmetry is clearly explained and the basic equations for copropagating fundamental and second-harmonic waves are simply derived. A detailed discussion, in terms of a phase-mismatch parameter, is given and the solutions of the coupled nonlinear equations are then analyzed in some detail. It is emphasized that only in certain circumstances can an analytical solution be found. In general, numerical analysis must be resorted to. The problem of determining the stability then arises. An averaged Lagrangian method is used for the stability analysis, based upon Gaussian trial functions. It is concluded that the interaction between the second-harmonic wave and the fundamental beam can be described in elegant mathematical terms and that the analysis is readily confirmed by exact numerical simulations. It is shown that it is convenient to discuss the two-beam interaction in terms of an "effective mass." It is then shown that the "mass" with linear phase-mismatch plane contains ranges in which the solitary waves can exist. In fact, it is fascinating that by combining the stability analysis, with the nonlinear phase-matching condition, very precise domains of stability can be found analytically. Finally, it is emphasized that the variational analysis reported here, together with the choice of trial function, is perfectly accurate when compared to the true dynamics, as revealed by the numerical simulations.

ACKNOWLEDGMENTS

K.X. wishes to thank EPSRC, the United Kingdom Engineering and Physical Sciences Research Council, for their generous support.

[1] G. P. Agrawal, *Nonlinear Fiber Optics* (Academic, Boston, 1989).
[2] A. D. Boardman and K. Xie, Phys. Rev. A **50**, 1851 (1994).
[3] A. D. Boardman, K. Xie, and A. A. Zharov, Phys. Rev. A **51**, 692 (1995).
[4] J. V. Moloney, A. C. Newell, and A. B. Aceves, Opt. Quantum Electron. **24**, 51 269 (1992).
[5] M. Schubert and B. Wilhelmi, *Nonlinear Optics and Quantum Electronics* (Wiley, New York, 1986).
[6] P. N. Butcher, *Nonlinear Optical Phenomena* (Ohio State Uni-

versity Engineering Publications, Columbus, 1965).
[7] R. DeSalvo, D. J. Hagan, M. Sheik-Bahae, G. I. Stegeman, and E. W. Van Stryland, Opt. Lett. **17**, 28 (1992).
[8] C. R. Menyuk, R. Schiek, and L. Torner, J. Opt. Soc. Am. B **11**, 2434 (1994).
[9] A. G. Kalocsai and J. W. Haus, Opt. Commun. **97**, 239 (1993).
[10] A. G. Kalocsai and J. W. Haus, Phys. Rev. A **49**, 574 (1994).
[11] W. E. Torruellas, G. Krijnen, D. Y. Kim, R. Schiek, and G. I. Stegeman, Opt. Commun. **112**, 122 (1994).
[12] G. Assanto, I. Torelli, and S. Trillo, Opt. Lett. **19**, 1720 (1994).
[13] R. Schiek, J. Opt. Soc. Am. B **10**, 1848 (1993).
[14] L. Torner, Opt. Commun. **114**, 136 (1995).
[15] L. Torner, C. R. Menyuk, and G. I. Stegeman, J. Opt. Soc. B (to be published).
[16] L. Torner, C. R. Menyuk, and G. I. Stegeman, J. Opt. Soc. B **12**, 889 (1995).
[17] A. V. Buryak and Y. S. Kivshar, Opt. Lett. **19**, 1612 (1994).
[18] A. V. Buryak and Y. S. Kivshar, Phys. Lett. A **197**, 407 (1995).
[19] K. Hayata and M. Koshiba, Phys. Rev. A **50**, 675 (1994).
[20] A. V. Buryak and Y. S. Kivshar, Phys. Rev. A **51**, R41 (1995).
[21] A. D. Boardman and K. Xie, Radio Sci. **28**, 891 (1993).
[22] G. B. Whitham, *Linear and Nonlinear Waves* (Interscience, New York, 1973).